Joint Optimization of Trajectory and Resource Allocation for Time-Constrained UAV-Enabled Cognitive Radio Networks

Yu Pan, Xinyu Da, Hang Hu, *Member, IEEE*, Yangchao Huang, Miao Zhang, *Member, IEEE*, Kanapathippillai Cumanan, *Senior Member, IEEE*, and Octavia A. Dobre, *Fellow, IEEE*

***Abstract*—Unmanned aerial vehicle (UAV)-enabled communication has emerged as an irreplaceable technology in military, disaster relief and emergency scenarios. This correspondence investigates the average throughput in a UAV-enabled cognitive radio network, where the UAV is regarded as a dedicated secondary user to enhance the network coverage and spectral efficiency. Based on the probabilistic line-of-sight channel, we exploit the joint design of UAV trajectory and resource allocation to maximize the average throughput under the constraints of co-channel interference and completion time. The original problem is a mixed integer non-convex problem which is generally NP-hard. We first decompose the primal problem into a bilevel programming problem, and then propose an efficient high-quality algorithm based on the particle swarm optimization approach. The optimized trajectory reveals the trade-off between throughput and co-channel interference. Numerical results verify the superiority of the proposed algorithm as compared to other benchmark schemes.**

***Index Terms*—Cognitive radio network, unmanned aerial vehicle (UAV) communication, trajectory design, throughput maximization.**

I. Introduction

Unmanned aerial vehicle (UAV)-enabled communication is considered as a promising technique to significantly improve the coverage and the performance of terrestrial communication networks. Due to their flexibility, UAVs can be deployed in many wireless communication scenarios, such as disaster relief and emergency communications [1]. Furthermore, UAVs are capable of providing reliable services in conventional communication systems. For example, they can support wireless services for users who are out of terrestrial network coverage [2].

Unfortunately, the spectrum scarcity problem of the UAV appears to be increasingly acute and urgent, which can be attributed to the current static spectrum allocation strategy [3] and the coexistence with other wireless devices (WDs). Thus, the cognitive radio (CR) technology, with the aim of addressing this challenge by dynamically sharing the spectrum resources, has been introduced to alleviate this problem. CR enables efficient dynamic spectrum access by allowing the UAVs to share the licensed spectrum bands without degrading the communication level of the primary network. Furthermore, the UAV-enabled CR communication networks have the additional advantages of strong line-of-sight (LoS) link and flexibility to deploy sensing nodes, when compared with the conventional CR networks.

Different UAV trajectory designs were investigated in the literature. One of the challenging issues is the limited on-board energy of UAVs [4], so the flying trajectory of the UAV was optimized to minimize the energy consumption, while satisfying the target throughput requirements of the ground nodes in [5]. To fully utilize the advantages of the UAV-enabled multicasting simultaneous wireless information and power transfer, the work in [6] jointly optimized the trajectory and transmit power to maximize the minimum achievable rate under the harvested energy constraints. A worst-case secrecy rate maximization problem was studied in [7] by jointly designing the three-dimensional (3D) trajectory and the time allocation under energy constraints. For throughput optimization, a joint trajectory and power control design was proposed in [8] under the constraints of flying speed, altitude, and collision avoidance. The problem was solved through employing the successive convex approximation with the first-order Taylor approximation in both [6] and [8]. However, the interference leakage to the primary receivers (PRs) and the probabilistic LoS channel were not taken into account, which introduce challenging problems in practice [9]. Thus, the above results on trajectory optimization cannot be applied to the UAV-enabled CR communication networks.

In our previous work [10], [11], throughput maximization was considered by jointly optimizing the sensing performance, the power allocation, and the UAV positions based on a circular trajectory. In [12], the robust trajectory and beamforming design were investigated in a downlink cognitive multiple-input single-output (MISO) UAV network. Since the aforementioned work only assumed the simplified LoS channel, which is inappropriate in urban communication scenario. The authors in [13] considered a more practically accurate angle-dependent Rician fading channel, where the UAV was employed to harvest sensing-data from distributed sensors.

Motivated by the aforementioned work in the literature, we investigate the throughput performance of a UAV-enabled CR network under a number of constraints. In particular, the contributions of our work can be summarized as follows: 1) We extend the communication system based on the probabilistic LoS channel, which approximates the occurrence of LoS and non-LoS (NLoS) channel as a logistic function, while most of the existing works have adopted the channel dominated by the LoS component; 2) The impact of the UAV's trajectory planning and resource allocation on efficient spectrum sharing is investigated, which reveals some insights for the trade-off between the UAV's throughput and the interference leakage to the PRs; 3) The corresponding optimization problem turns out to be challenging, which is formulated as a mixed

Manuscript received September 7, 2021; revised January 12, 2022; accepted February 10, 2022. Date of publication February 16, 2022; date of current version May 20, 2022. The work of Hang Hu was supported in part by the National Natural Science Foundation of China under Grant 61901509 and in part by the President Foundation of Air Force Engineering University under Grant XZJK2019033. The work of Miao Zhang was supported in part by the National Natural Science Foundation of China under Grant 62101080 and in part by the Science and Technology Research Program of Chongqing Municipal Education Commission of China under Grant KJQN202100738. The work of Octavia A. Dobre was supported by the Natural Sciences and Engineering Research Council of Canada (NSERC) through its Discovery program. The review of this article was coordinated by Dr. Kaigui Bian. *(Corresponding author: Xinyu Da.)*

Yu Pan is with Graduate College, Air Force Engineering University, Xi'an 710077, China (e-mail: panyu@mail.nwpu.edu.cn).

Xinyu Da is with the College of Artificial Intelligence, Yango University, Fuzhou 350015, China (e-mail: kgddxy2008@163.com).

Hang Hu and Yangchao Huang are with Information and Navigation College, Air Force Engineering University, Xi'an 710077, China (e-mail: xd_huhang@126.com; gxyxhbwhyc@sohu.com).

Miao Zhang is with the School of Information Science and Engineering, Chongqing Jiaotong University, Chongqing 400074, China (e-mail: msczz@foxmail.com).

Kanapathippillai Cumanan is with the Department of Electronic Engineering, University of York, New York YO10 5DD, U.K. (e-mail: kanapathippillai.cumanan@york.ac.uk).

Octavia A. Dobre is with the Department of Electrical and Computer Engineering, Memorial University, St. John's, NL A1B 3X5, Canada (e-mail: odobre@mun.ca).

Digital Object Identifier 10.1109/TVT.2022.3151671

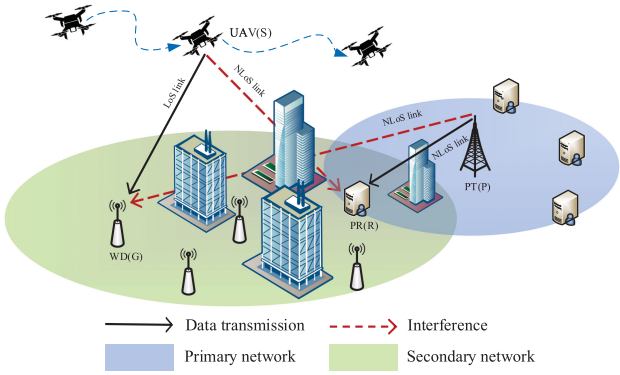

Fig. 1. A UAV-enabled underlay CR communication network in highrise urban environment.

integer non-convex problem. We transform the original problem into an equivalent two-stage problem, and develop an optimal solution with the particle swarm optimization algorithm based on decomposition, by applying pre-programmed location (PPL-PSO/D); 4) Numerical results confirm the accuracy of the analytical results and validate the superiority of the proposed algorithm.

II. System Model

Consider the downlink transmission in a UAV-enabled CR communication network, where the UAV is dispatched as a monitor to fly along the scheduled trajectory and transmit monitoring data to the ground WDs. As illustrated in Fig. 1, the secondary network is composed of one UAV and M ground WDs denoted by S and G_m $(m \in \mathcal{M} = \{1, \ldots, M\})$, respectively. The primary network is composed of one primary transmitter (PT) and K PRs (with uncertain region), denoted by P and R_k $(k \in \mathcal{K} = \{1, \ldots, K\})$, respectively. The locations of the WDs and PT are assumed to be known to the UAV a priori for its trajectory design [14]. Specifically, we adopt the underlay mode in this CR network, such that the UAV can access the licensed spectrum simultaneously with the primary network while ensuring the required quality-of-service (QoS) of PRs [15]. The goal of the scheme is to transmit as much monitoring data as possible under the co-channel interference constraint during a certain time period, so the fairness of all WDs is sacrificed for performance improvement. The UAV is equipped with global positioning system (GPS) and hence its dynamic locations can be easily obtained.

The UAV is assumed to complete the flight within T_{tot} seconds, which is equally divided into N time slots, and the duration of each time slot is T_s seconds. In each n-th time slot, the UAV's projected location onto the horizontal plane is denoted by $\boldsymbol{Q}[n] \in \mathbb{R}^{2\times 1}$ in a 3D Cartesian coordinate system, where $n \in \mathcal{N} = \{1, \ldots, N\}$. Then, the distance between the UAV and the m-th ground WD is given by $d_{SG}^{m}[n] = \sqrt{h^2 + \|\boldsymbol{Q}[n] - \mathbf{g}_m\|^2}$. The horizontal locations of the WDs are given by $\mathbb{G} = \{\boldsymbol{g}_1, \ldots, \boldsymbol{g}_M\}^{\mathrm{T}}$, with $\boldsymbol{g}_m \in \mathbb{R}^{2\times 1}$. Two types of channel are distinguished in this system, namely ground-to-ground (G2G) channel and air to ground (A2G) channel. In order to capture practical scenarios, the A2G channel considers stochastic shadowing based on the probabilistic LoS link, where the large-scale fading is modeled as a random variable based on the occurrence probabilities of LoS and NLoS links. The channel gain between node u and another node v can be expressed as

$$h_{uv}^{\mathrm{L}} = \tilde{g}_{uv} \left(\mathrm{PL}_{uv}^{\mathrm{LoS}}\left(d_{uv}\right)\right)^{-\frac{1}{2}}, \tag{1}$$

$$h_{uv}^{\mathrm{N}} = \tilde{g}_{uv} \left(\mathrm{PL}_{uv}^{\mathrm{NLoS}}\left(d_{uv}\right)\right)^{-\frac{1}{2}}, \tag{2}$$

where $\mathrm{PL}_{uv}^{\mathrm{LoS}}$ and $\mathrm{PL}_{uv}^{\mathrm{NLoS}}$ denote the pathloss for LoS and NLoS links, respectively. The parameter d_{uv} is the distance between node u and v, and $\tilde{g}_{uv}$ is the normalized channel vector with $\mathrm{E}[|\tilde{g}_{uv}|^2] = 1$. Moreover, the small-scale fluctuations are ignored in this paper, since the trajectory of UAV is mainly designed in an off-line manner, and is not aimed to cater to the small-scale fading that usually varies randomly as well as more rapidly over space when compared to large-scale channel power gains [15]. The average pathloss for LoS and NLoS links are given by [16]:

$$\mathrm{PL}_{uv}^{\mathrm{LoS}}(\mathrm{dB}) = \lg\left(\frac{4\pi f d_{uv}}{c}\right) + \xi_{\mathrm{LoS}}, \tag{3}$$

$$\mathrm{PL}_{uv}^{\mathrm{NLoS}}(\mathrm{dB}) = \lg\left(\frac{4\pi f d_{uv}}{c}\right) + \xi_{\mathrm{NLoS}}, \tag{4}$$

where ξ_{LoS} and ξ_{NLoS} denote the average additional propagation loss for LoS and NLoS links, respectively. f is the carrier frequency and c is the speed of light. The probability of the LoS link for the m-th WD in the n-th time slot is given by $p_m^{\mathrm{LoS}}[n]$, which generally depends on the propagation environment and the elevation angle θ between the UAV and ground nodes. Therefore, $p_m^{\mathrm{LoS}}[n]$ is expressed as

$$p_m^{\mathrm{LoS}}[n] = \frac{1}{1 + \alpha \exp[-\beta(\theta_m[n] - \alpha)]}, \tag{5}$$

where α and β are constant values determined by the propagation environment, and the elevation angle (in degrees) can be calculated as

$$\theta_m[n] = \frac{180}{\pi} \arcsin\left(\frac{h}{d_{\mathrm{SG}}^{m}[n]}\right). \tag{6}$$

Considering the UAV-WD scheduling, we employ a binary variable $\lambda_m[n] \in \{0, 1\}$ to characterize the allocation strategy in the n-th time slot: $\lambda_m[n] = 1$ indicates that the m-th WD is woken up to communicate with the UAV, otherwise, $\lambda_m[n] = 0$. Since the UAV communicates with the ground WDs under the time-division multiple access (TDMA) mode, we can obtain

$$\sum_{m=1}^{M} \lambda_m[n] \le 1, \quad \forall n \in \mathcal{N}. \tag{7}$$

In each time slot, the transmission power allocated to the UAV to be optimized is given by $P[n]$, the transmission power of the PT is given by P_{P}, and the received power at the PR can be defined as $P_{\mathrm{P}}|h_{\mathrm{PR}}^{N}|^2$. The protected boundary is defined due to the uncertainty of the location information of PR, which is denoted by L^* and this can ensure the QoS of the primary network. L^* is determined by the signal-to-noise radio (SNR) threshold γ^{th} of the PR, which satisfies $\frac{P_{\mathrm{P}}|h_{\mathrm{PR}}^{\mathrm{N}}|^2}{\sigma^2} \ge \gamma^{\mathrm{th}}$ (σ^2 is the noise power at the PR). The deployment of the PRs is generally random and unknown; hence, we assume that the PR is located on the protected boundary such that its QoS can be guaranteed. The constraint on the outage threshold is given as

$$\frac{P[n]\left(p_{\mathrm{SR}}^{\mathrm{LoS}}[n]\left|h_{\mathrm{SR}}^{\mathrm{L}}\right|^2 + p_{\mathrm{SR}}^{\mathrm{NLoS}}[n]\left|h_{\mathrm{SR}}^{\mathrm{N}}\right|^2\right) + \sigma^2}{P_{\mathrm{P}}\left|h_{\mathrm{PR}}^{\mathrm{N}}\right|^2} \le \theta_{\mathrm{out}}, \tag{8}$$

where $p_{\mathrm{SR}}^{\mathrm{LoS}}[n]$ is the probability of the LoS link between the m-th UAV and the PR in the n-th time slot, and θ_{out} is the outage threshold.

III. Problem Formulation and Proposed Solution

A. Problem Formulation

In this section, we formulate the design problem to maximize the average throughput of the UAV over all time slots. Based on the system model in the previous section, the expectation of the system throughput in the n-th time slot can be derived as

$$\mathbb{E}\left(R_m[n]\right) = \pi_0 \mathbb{E}\left(\bar{R}_m[n]|i=0\right) + \pi_1 \mathbb{E}\left(\bar{R}_m[n]|i=1\right), \quad (9)$$

where $i \in \mathcal{I} = \{0,1\}$, and $i=1$ represents the case that the actual state of PT is present, otherwise $i=0$. π_1 is the probability of the existence of PT and π_0 is the probability of the absence of PT. The mathematical expectation of the throughput between the UAV and the m-th WD denoted by $\mathbb{E}(\bar{R}_m[n])$ is given by

$$\mathbb{E}\left(\bar{R}_m[n]\right) = p_m^{\mathrm{LoS}}[n] R_m^{\mathrm{L}}[n] + p_m^{\mathrm{NLoS}}[n] R_m^{\mathrm{N}}[n], \quad (10)$$

where $R_m^{\mathrm{L}}[n]$ and $R_m^{\mathrm{N}}[n]$ are the throughput between the UAV and the m-th WD in LoS and NLoS links, respectively, which can be calculated as

$$R_m^{\mathrm{L}}[n] = \begin{cases} B\log_2\left(1+\frac{P_m[n]\left|h_{\mathrm{SG}}^{\mathrm{L}}\right|^2}{\sigma^2}\right), & i=0 \\ B\log_2\left(1+\frac{P_m[n]\left|h_{\mathrm{SG}}^{\mathrm{L}}\right|^2}{\sigma^2+P_{\mathrm{P}}\left|h_{\mathrm{PG}}^{\mathrm{N}}\right|^2}\right), & i=1 \end{cases} \quad (11)$$

$$R_m^{\mathrm{N}}[n] = \begin{cases} B\log_2\left(1+\frac{P_m[n]\left|h_{\mathrm{SG}}^{\mathrm{N}}\right|^2}{\sigma^2}\right), & i=0 \\ B\log_2\left(1+\frac{P_m[n]\left|h_{\mathrm{SG}}^{\mathrm{N}}\right|^2}{\sigma^2+P_{\mathrm{P}}\left|h_{\mathrm{PG}}^{\mathrm{N}}\right|^2}\right), & i=1. \end{cases} \quad (12)$$

where the signal bandwidth is denoted by B. As the UAV's location and the probability of the LoS link are time-varying, we consider the average throughput over all time slots, which can be defined as

$$\tilde{R} = \sum_{n=1}^{N}\sum_{m=1}^{M} \frac{\lambda_m[n]\mathbb{E}\left\{R_m[n]\right\}}{N}. \quad (13)$$

In this correspondence, we jointly optimize the UAV-WD scheduling $\lambda_m[n]$, the transmission power allocation $P[n]$, and the UAV trajectory $\boldsymbol{Q}[n]$. The objective is to maximize the average throughput of the UAV under the constraints of the completion time, maximum speed, and outage threshold. Therefore, the original problem can be formulated as

$$(\mathbf{P1}) \quad \max_{\boldsymbol{Q}[n],\lambda_m[n],P[n]} \quad \tilde{R} \quad (14a)$$

$$\text{s.t.} \quad T \le T_{\mathrm{tot}}, \quad (14b)$$

$$\|\boldsymbol{Q}[n+1]-\boldsymbol{Q}[n]\| \le v_{\max}\cdot T_{\mathrm{s}}, \quad (14c)$$

$$\frac{P_{\mathrm{P}}\left|h_{\mathrm{PR}}^{\mathrm{N}}\right|^2}{\sigma^2} \ge \gamma^{\mathrm{th}}, \quad (14d)$$

$$(7),\ (8), \quad (14e)$$

where T_{tot} is the maximum mission completion time, $\boldsymbol{Q}[0] = \boldsymbol{Q}_{\mathrm{I}}$, $\boldsymbol{Q}[N+1] = \boldsymbol{Q}_{\mathrm{F}}$, and $\boldsymbol{Q}_{\mathrm{I}}$ and $\boldsymbol{Q}_{\mathrm{F}} \in \mathbb{R}^{2\times 1}$ represent the UAV's initial and final projected locations on the horizontal plane.

B. A Two-Stage PPL-PSO/D Algorithm to Solve Problem $(\mathbf{P1})$

Problem $(\mathbf{P1})$ is a mixed integer non-convex optimization problem, where the binary discrete variable $\lambda_m[n]$ defined in (7) and the discrete trajectory of the UAV ($\boldsymbol{Q}[n]$) in (14c) impose several non-convex constraints. Therefore, we utilize the PPL-PSO/D algorithm to determine the optimal solution. To make the problem tractable, we first convert it into a bilevel problem, which first solves the UAV-WD scheduling problem. The inner problem can be written as

$$(\mathbf{P2.1}) \quad \max_{\lambda_m[n]} \quad \hat{R}[n] = \sum_{m=1}^{M} \lambda_m[n]\mathbb{E}\left\{R_m[n]\right\} \quad (15a)$$

$$\text{s.t.} \quad (14\,\mathrm{d}), (14\mathrm{e}). \quad (15b)$$

As can be seen, the inner problem $(\mathbf{P2.1})$ is a single-variable integer problem, which can be easily solved through exhaustive enumeration, and the solution is given by $\hat{R}_{\max}[n]$. As the locations of the UAV are time-varying, the value of $\lambda_m[n]$ is also varying over time. The decomposition by $(\mathbf{P2.1})$ and $(\mathbf{P2.2})$ enables the tractability of this optimization problem. Then, the outer problem to optimize the UAV trajectory and power allocation can be defined as

$$(\mathbf{P2.2}) \quad \max_{\boldsymbol{Q}[n],P[n]} \quad \tilde{R} = \sum_{n=1}^{N} \frac{\hat{R}_{\max}[n]}{N} \quad (16a)$$

$$\text{s.t.} \quad (14\mathrm{b}), (14\mathrm{c}). \quad (16b)$$

The proposed iterative algorithm to solve this two-stage problem is based on the PSO algorithm with pre-programmed locations, which can obtain the approximated optimal trajectory $\boldsymbol{Q} \in \mathbb{R}^{2\times N}$.

The search space in problem $(\mathbf{P2.1})$ is $2N$-dimensional and the generation matrix is given by $\mathbb{X} = \{\boldsymbol{x}_1^t, \boldsymbol{x}_2^t \ldots \boldsymbol{x}_A^t\}^{\mathrm{T}}$, where A is the population size of the particle swarm and t is the iteration times. Thus, $\boldsymbol{x}_a^t \in \mathbb{R}^{1\times 2N}$ corresponds to the a-th particle's location at the t-th iteration. Considering the constraint (14c), we pre-programmes the particle location $\boldsymbol{x}_a^t$ as

$$\boldsymbol{x}_a^t(i) = \begin{cases} \frac{a+1-g(i)}{A+1}\boldsymbol{Q}_{\mathrm{I}}(1) + \frac{g(i)}{A+1}\boldsymbol{Q}_{\mathrm{F}}(1), & i=2n+1, \\ \frac{a+1-g(i)}{A+1}\boldsymbol{Q}_{\mathrm{I}}(2) + \frac{g(i)}{A+1}\boldsymbol{Q}_{\mathrm{F}}(2), & i=2n, \end{cases} \quad (17)$$

where $g(i) = \lfloor \frac{i+1}{2} \rfloor$, with $\lfloor(\cdot)\rfloor$ denoting the floor operation. The fitness value will be computed as F_a^t in each iteration, which is determined by the average communication throughput $\tilde{R}$ and the penalty function $g(\boldsymbol{x}_a^t)$ for constraint (14c). The expression of $F(\boldsymbol{x})$ and $g(\boldsymbol{x})$ are given as

$$F(\boldsymbol{x}) = \sum_{n=1}^{N} \hat{R}_{\max}[n] + g(\boldsymbol{x}), \quad (18)$$

$$g(\boldsymbol{x}) = \sum_{n=0}^{N} \xi \cdot \max(0, \|\boldsymbol{Q}[n+1]-\boldsymbol{Q}[n]\| - v_{\max}T_{\mathrm{s}}), \quad (19)$$

where the value of ξ is assumed to be a large negative number. For each swarm, the optimal particle location is updated as $\boldsymbol{q}_a^t$ with its fitness value denoted by y_a^t. Consequently, the global optimum particle $\boldsymbol{q}^*$ can be achieved, which provides the maximum average throughput y^*. Since the fitness value of $\mathbf{P1}$ remains monotone non-decreasing after each iteration, and is upperbounded by a finite value, the proposed algorithm is guaranteed to converge. The proposed PPL-PSO/D algorithm also considers the inertia weight ω as a variable to enhance the algorithm performance. The details of the improved PPL-PSO/D algorithm are provided in Algorithm 1, where $\boldsymbol{\Psi}$ and $\boldsymbol{\Phi}$ are two matrices with the elements randomly distributed $\in [0,1]$, and $t_{\max}$ represents the maximum iteration number.

IV. Numerical Results

In this section, numerical results are provided to validate the performance of our proposed algorithm. The channel model has been

Algorithm 1: PLL-PSO/D algorithm for average throughput maximization.

Initialize the location matrix $\mathbb{X} = \{\boldsymbol{x}_1^t, \boldsymbol{x}_2^t \dots \boldsymbol{x}_A^t\}^T$ by formula (17), $y_a^t = 0$, $y^* = \max\{y_a^t; a = 1, \dots, A\}$, and $t = 0$;
while $t < t_{\max}$ **do**
  for $n = 1 : N$
  $\omega = 1.4 - \frac{0.4t}{t_{\max}}$, $c_1 = 2$, $c_2 = 2$;
  $\boldsymbol{v}_a^{t+1}(n) = \omega \boldsymbol{v}_a^t(n) + c_1 \boldsymbol{\Psi}^t(\boldsymbol{q}_a^t(n) - \boldsymbol{x}_a^t(n)) + c_2 \boldsymbol{\Phi}^t(\boldsymbol{q}_*^t(n) - \boldsymbol{x}_a^t(n))$;
  $\boldsymbol{x}_a^{t+1}(n) = \boldsymbol{x}_a^t(n) + \boldsymbol{v}_a^{t+1}(n)$;
  for $a = 1 : A$
  Compute the fitness value of $x_a^t(n)$;
  Update the optimal fitness value y_a^t and the global fitness value y^*;
  Update the optimal population particle $\boldsymbol{q}_a^t$ and the global particle $\boldsymbol{q}^*$;
  end for
  end for
  $t = t + 1$;
end while

described in Section II. The simulation parameters are set as follows: $A = 1000, t_{\max} = 2 \times 10^4, B = 10^5$ Hz [11], $P_{\rm P} = 30$ dB, $\sigma^2 = -78$ dBm, $\mathbb{G} = [-50, -300; 50, 150; 100, 0]$, $N = 15$, $f = 2.44$ GHz, and $v_{\max} = 18$ m/s. In accordance to the Federal Aviation Administration regulation, the altitude of the UAV is $h = 100$ m. As for the general highrise urban environment, the parameters are set as $\alpha = 25$, $\beta = 0.112, \xi_{\rm LoS} = 2.3$ dB and $\xi_{\rm NLoS} = 34$ dB. Regarding the underlay mode of the CR network, we adopt $\pi_1 = 0.7$, $\gamma^{\rm th} = 5.5$ dB and $\theta_{\rm out} = -28$ dB.

In Fig. 2, the optimal UAV's trajectories with joint optimization and separate optimization are presented. The separate optimization indicates that the trajectory is first optimized without power allocation, and the differences between the trajectories are analyzed as follows. Generally, the UAV can achieve the maximum throughput when it flies above the WD, so in all cases the UAV tends to fly towards the ground WDs during its flight from $Q_{\rm I}$ to $Q_{\rm F}$. When the completion time is not sufficient (e.g., $T_{\rm tot} = 35$ s), it should first satisfy the time constraint, and hence, it can only approach slightly the WDs and accomplish the mission at the expense of lower throughput. When longer completion time is allocated (e.g., $T_{\rm tot} = 50$ s), the UAV flies around $\rm WD_3$ at a slower speed (nearly static) to achieve better channel gain. However, for separate optimization in Fig. 2(b), the UAV will not fly away from the primary network to alleviate the co-channel interference. Consequently, the proposed joint optimization algorithm achieves the optimum throughput under co-channel interference and time constraints.

Fig. 3 shows the power allocation and communication scheduling of the UAV while the location information of PRs is uncertain. Obviously, in both Fig. 3(a) and Fig. 3(b), the transmission power decreases more when it approaches $\rm WD_2$ to guarantee the QoS of PRs. This is also the reason that the UAV tends to fly closer to $\rm WD_1$ rather than $\rm WD_2$ in the cases with $T_{\rm tot} = 50$ s and $T_{\rm tot} = 45$ s in Fig. 3(a). When the UAV flies towards $\rm WD_2$, it will also approach the primary network. The maximum transmission power of the UAV will be reduced due to the constraint in (8), although the decreasing distance improves the channel gain. The compromised trajectory in Fig. 3(a) reflects the trade-off between increasing the channel gain and decreasing the

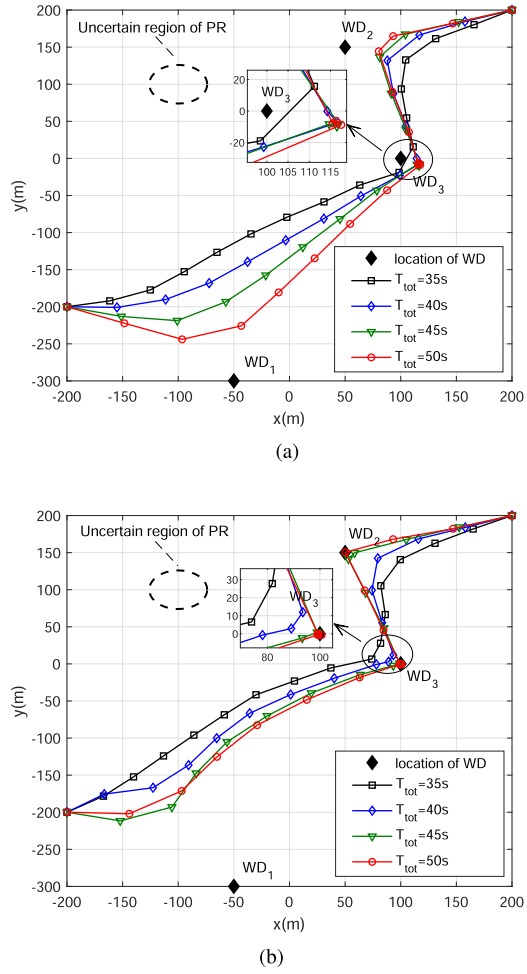

Fig. 2. The optimized UAV trajectories versus different mission completion times. (a) Joint optimization. (b) Separate optimization.

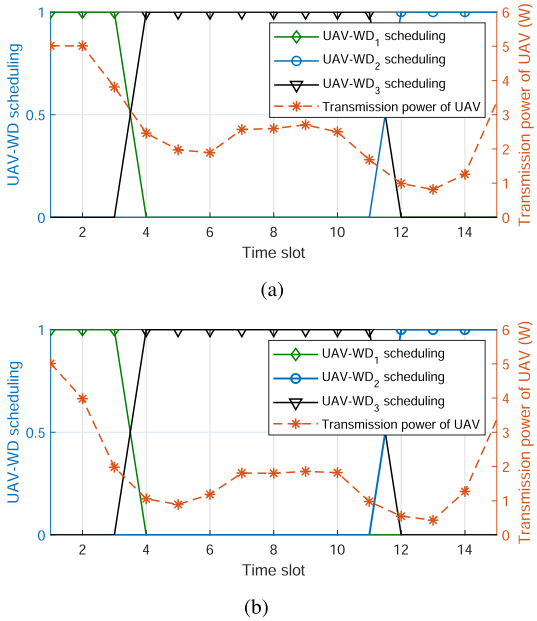

Fig. 3. The optimal UAV-WD scheduling and transmission power $P[n]$ with $T_{\rm tot} = 50$ s. (a) Joint optimization. (b) Separate optimization.

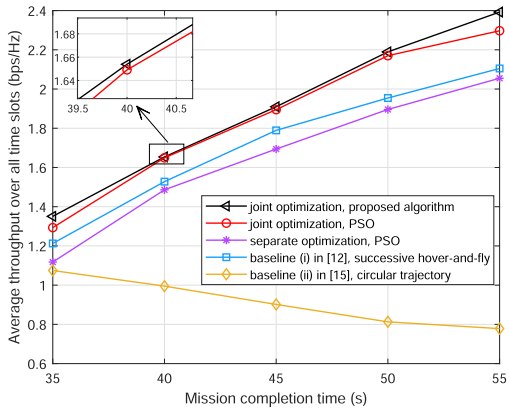

Fig. 4. Comparison of average throughput of different schemes.

power allocation. For separate optimization in Fig. 3(b), as expected, the UAV directly flies over WD_2, with less power allocation and worse throughput performance.

Finally, Fig. 4 compares the proposed trajectory design with several alternative benchmark schemes in terms of throughput performance. Two baseline schemes are considered: i) the UAV performs successively hover-and-fly as in [14]; and ii) the UAV trajectory is set to be a circular trajectory with a constant speed, which is centered at the geometric mean of the users' locations as in [17]. Since simulation results reveal that the average throughput generally converges within 6000 iterations, we set $A = 1000$ and $t_{\max} = 6000$. It is firstly observed from Fig. 4 that the separate optimization cannot achieve a similar performance as joint optimization. On the other hand, the baseline (i) outperforms the separate optimization, which is expected as it adaptively optimizes the hovering locations considering the power allocation. The baseline (ii) performs worst and its throughput decreases with increasing T_{tot}. The reason for this is that increasing the radius also increases its distance to WD and co-channel interference to PR, which is proved impractical in this UAV-enabled CR network. As expected, the proposed trajectory design significantly outperforms all four benchmark schemes, and the comparison will provide important insights to incorporate in the efficient system design.

V. Conclusion

In this correspondence, the principle of spectrum sharing has been applied to the UAV-enabled communications, and the average throughput with uncertain locations of PR has been investigated. Under the constraint of severe interference to co-channel terrestrial WDs, we have exploited the optimal UAV trajectory, communication scheduling and power allocation in the probabilistic LoS channel, and achieved the performance improvement of the UAV secondary network. The original non-convex throughput maximization problem has been decomposed into a two-stage problem, and the proposed PPL-PSO/D algorithm has efficiently achieved the trade-off between maximizing the throughput and minimizing the co-channel interference. Analytical and numerical results have been provided to validate the superior performance of our proposed design.

References

[1] H. Baek and J. Lim, "Design of future UAV-relay tactical data link for reliable UAV control and situational awareness," *IEEE Commun. Mag.*, vol. 56, no. 10, pp. 144–150, Oct. 2018.

[2] F. Zhou, Y. Wu, H. Sun, and Z. Chu, "UAV-enabled mobile edge computing: Offloading optimization and trajectory design," in *Proc. IEEE Int. Conf. Commun.*, 2018, pp. 1–6.

[3] J. Hu, H. Zhang, and L. Song, "Reinforcement learning for decentralized trajectory design in cellular UAV networks with sense-and-send protocol," *IEEE Internet Things J.*, vol. 6, no. 4, pp. 6177–6189, Aug. 2019.

[4] W. Wang *et al.*, "Energy-constrained UAV-assisted secure communications with position optimization and cooperative jamming," *IEEE Trans. Commun.*, vol. 68, no. 7, pp. 4476–4489, Jul. 2020.

[5] Y. Zeng, J. Xu, and R. Zhang, "Energy minimization for wireless communication with rotary-wing UAV," *IEEE Trans. Wireless Commun.*, vol. 18, no. 4, pp. 2329–2345, Apr. 2019.

[6] J. -M. Kang and C. -J. Chun, "Joint trajectory design, Tx power allocation, and Rx power splitting for UAV-Enabled multicasting SWIPT systems," *IEEE Syst. J.*, vol. 14, no. 3, pp. 3740–3743, Sep. 2020.

[7] W. Wang *et al.*, "Robust 3D-Trajectory and time switching optimization for Dual-UAV-Enabled secure communications," *IEEE J. Sel. Areas Commun.*, vol. 39, no. 11, pp. 3334–3347, Nov. 2021.

[8] C. Shen, T. Chang, J. Gong, Y. Zeng, and R. Zhang, "Multi-UAV interference coordination via joint trajectory and power control," *IEEE Trans. Signal Process.*, vol. 68, pp. 843–858, Jan. 2020, doi: 10.1109/TSP.2020.2967146.

[9] Y. Huang, W. Mei, J. Xu, L. Qiu, and R. Zhang, "Cognitive UAV communication via joint maneuver and power control," *IEEE Trans. Commun.*, vol. 67, no. 11, no. 11, pp. 7872–7888, Nov. 2019.

[10] H. Hu, Y. Huang, X. Da, H. Zhang, L. Ni, and Y. Pan, "Optimization of energy management for UAV-enabled cognitive radio," *IEEE Wireless Commun. Lett.*, vol. 9, no. 9, pp. 1505–1508, Sep. 2020.

[11] H. Hu *et al.*, "Optimization of energy utilization in cognitive UAV systems," *IEEE Sens. J.*, vol. 21, no. 3, pp. 3933–3943, Feb. 2021.

[12] B. Liu, Y. Wan, F. Zhou, Q. Wu, and R. Q. Hu, "Robust trajectory and beamforming design for cognitive MISO UAV networks," *IEEE Wireless Commun. Lett.*, vol. 10, no. 2, pp. 396–400, Feb. 2021.

[13] C. You and R. Zhang, "3D trajectory optimization in Rician fading for UAV-enabled data harvesting," *IEEE Trans. Wireless Commun.*, vol. 18, no. 6, pp. 3192–3207, Jun. 2019.

[14] J. Xu, Y. Zeng, and R. Zhang, "UAV-Enabled wireless power transfer: Trajectory design and energy optimization," *IEEE Trans. Wireless Commun.*, vol. 17, no. 8, pp. 5092–5106, Aug. 2018.

[15] F. Zhou, N. C. Beaulieu, Z. Li, J. Si, and P. Qi, "Energy-effcient optimal power allocation for fading cognitive radio channels: Ergodic capacity, outage capacity, and minimum-rate capacity," *IEEE Trans. Wireless Commun.*, vol. 15, no. 4, pp. 2741–2755, Apr. 2016.

[16] A. Al-Hourani, S. Kandeepan, and S. Lardner, "Optimal LAP altitude for maximum coverage," *IEEE Wireless Commun. Lett.*, vol. 3, no. 6, pp. 569–572, Dec. 2014.

[17] Q. Wu, Y. Zeng, and R. Zhang, "Joint trajectory and communication design for Multi-UAV enabled wireless networks," *IEEE Trans. Wireless Commun.*, vol. 17, no. 3, pp. 2109–2121, Mar. 2018.